SAM-PIE: SAM-Enabled Photovoltaic-Module Image Enhancement for Fault Inspection and Analysis Using ResNet50 and CNNs

SAM-Enabled Photovoltaic-Module Image Enhancement (SAM-PIE)

Rotimi-Williams Bello*, Pius A. Owolawi, Etienne A. van Wyk, Chunling Du
Department of Computer Systems Engineering-Faculty of Information and Communication Technology,
Tshwane University of Technology, South Africa

***Abstract*—Different models have been developed for segmentation tasks, each with its uniqueness. Recently, the Segment Anything Model (SAM) was added to the pool of these models with expectations of addressing their weaknesses. SAM, although trained on a huge dataset for segmentation of anything, particularly images of natural source, produces suboptimal results when applied to segmentation of photovoltaic module image due to difference in semantic between photovoltaic module and natural images. In spite of the current suboptimal performance of SAM in segmentation of photovoltaic module images, it demonstrates detection and identification of thermal anomalies in photovoltaic module images that majorly contribute to power production loss. The implication of this is that, the task, the model, and the data corresponding to SAM are applicable to photovoltaic module image diagnosis. In this paper, we propose SAM-enabled photovoltaic-module image enhancement (SAM PIE) for fault inspection and analysis using ResNet50 and CNNs. SAM-PIE combines the strength of SAM for enhancement of the fault inspection and analysis procedure, for optimal performance of the proposed method. Experiments were performed on three thermal anomaly image datasets of photovoltaic modules to validate the performance of SAM-PIE for the classification tasks. The results obtained validates the potential capability of SAM-PIE to perform photovoltaic module image classification. The dataset is publicly and freely available for scientific community use at https://doi.org/10.17632/5ssmfpgrpc.1**

***Keywords*—Anomaly; convolution neural networks; crack; hotspot; photovoltaic; Residual Network-50; shading**

I. INTRODUCTION

Recently, there was an emergence of a state-of-the-art foundational model called the Segment Anything Model (SAM) [1] in the field of Computer Vision (CV) for image segmentation tasks. The main components that make the leap possible for the SAM are: (a) Prompts for new segmentation task, (b) SAM's model, and (c) SA-1B dataset. The prompt-able segmentation task was proposed in order to return a valid segmentation mask provided any prompt for segmentation is given. The main task of the prompt is simply to specify the image's object to segment, e.g., spatial or text information can be a prompt for object identification. For an output mask to be valid, there is a requirement that the output under any circumstances (for example, when there is an ambiguity in what object a prompt specifies in an image) should generate sensible mask at the least for one of the objects in the image.

The innovative design of the SAM model satisfies all the constraints imposed on the model architecture due to prompt-able task of segmentation and reality in real-world applications. In particular, prompts flexibility support masks computation in amortized real-time and ambiguity-aware [1-2]. Based on the abovementioned qualities attributed to SAM and its demonstration as a good model trained on a wide-ranging scalable data for flexibility, studies reveal the tendency of it facing challenges in tasks involving domain-specific segmentation solution [3], as noticed in some photovoltaic (PV) module image segmentation scenarios [4-6]. The rise of PV power has given a new dimension to renewable energy as evident in the global renewable energy, and this trend continues in gaining more acceptance as alternative to power generation [7-12].

The PV explosion requires an in-depth knowledge of its widespread, challenges, and prospect for concern individuals [13-15]; and this knowledge is essential for its proper monitoring, management, and maintenance across borders [16-20]. The inspection, detection, identification, and analysis of faults in PV installations have greatly been enhanced by the progress made in CV [21-24]. However, the majority of research on PV installations concentrate on using conventional CV techniques for inspection and analysis of the anomalies in solar cells of PV modules, which performs below expectations [25-27]. Moreover, high-resolution images are extremely required to obtain accurate inspection and analysis of PV modules [28], and the conventional techniques pose challenges regarding this.

Many researchers have attributed the inaccuracy obtained in their segmentation tasks to incapability of SAM when applied to PV image segmentation tasks, confirming the discrepancies in the tasks, model, and datasets. Although SAM shows segmentation efficiency in object-specific tasks, it still has limitations when dealing with fine structures, small disconnected components, weak boundaries and modalities [29-30]. Complex modalities, fine modular structures, small disconnected cell components, and absence of sharp boundaries are the challenges confronting SAM in PV image segmentation [28]. Additionally, the segment anything-1

The authors received funding from the Tshwane University of Technology, South Africa.

billion (SA-1B) of natural images on which SAM was pre-trained couple with the approach to determine boundaries based on discrepancy in intensity [28] is not applicable to PV images due to analysis of solar cells of the PV modules.

Moreover, while SAM can carry out many tasks, it does not have the prompts capability for panoptic and semantic segmentation implementation. Lately, SAM has experienced so much improvement due to many studies commitment to enhancing it due to its disappointing results to suit domain-specific tasks as noticed in PV image analysis. Several of these studies has dedicated their strength to fine-tuning the SAM model to enhance its performance and reliability for PV image analysis. Yang et al. [13] in their quest to meet the demand for the extraction of large-scale PV panel, proposed a novel weakly-supervised method that was based on the SAM model. Knowing the importance of broad data volumes and the knowledge that the extraction process requires the concept of latent PV locations for reduction in scope of the amount processed subsequently, they applied the method to the segmentation of latent PV locations for smooth passage from classification to segmentation. They achieved segmentation results that could stand the test of time.

Although SAM being initialized with a self-supervised technique [28], its efficiencies depend on large-scale supervised training. Rafaeli et al. [2] addressed this issue by proposing segmentation that is prompt-based at varied light conditions and resolutions using SAM 2. Their study revealed the efficiency of SAM 2 over SAM, particularly when prompted by points under lighting conditions that are sub-optimal. SAM's strength is challenged in segmentation of PV images, being a model trained on massive natural images. Although SAM may be prompt-able to efficiently segment PV images, it can still differentiate conspicuous solar cells of PV modules according to changes in image pixels. PV images are images of solar panels with a lot of revealing information only under high thermal image and pixel resolutions [31-32].

Therefore, thermal captured and enhanced images give visual quality to PV images for valuable information on anomalies detection, and analysis beyond what can be obtained from original image. Based on this, the aim of applying the techniques of PV image enhancement (PIE) in this study is to attain efficient and excellent inspection and analysis of PV faults from the available original PV imagery [33]. Therefore, we propose a new SAM-based PIE method (SAM-PIE) with the sole aim of enhancing the inspection and analysis of PV image segmentation models, and giving different perspective to the potential value of SAM in PV image analysis.

Under moderate prompts, the stability scores and masks generated by SAM are essential resource for PV image segmentation and analysis. An important factor that distinguished SAM-PIE from the traditional IE methods is the low-level in which the traditional IE methods frequently work, which is below the high-level requirement for reconstructing and recovering an original image [5], which is what SAM-PIE aims to achieve. This feat by SAM-PIE was attained by increasing semantic structures from SAM. Our proposed image enhancement method, SAM-PIE is easy to adapt to SAM, ensuring its applicability in solving anomalies in solar cells of PV modules by PV experts. In this paper, two classification models, ResNet50 [34] and Convolutional Neural Networks (CNNs), popular for their applications in PV image segmentation tasks were selected for the evaluation of SAM-PIE. One thousand PV module datasets [35], a Mendeley data comprising Hotspots (350 thermal generated images), Cracks (350 thermal generated images) and Shadings (300 thermal generated images) were used in performing the image segmentation experiments.

Research reveals that prior maps generated from effect of adding together the original and SAM's generated images can be employed for network inputs enhancement and thus improving the efficiency and performance of downstream models developed for segmenting PV images. This revelation motivated us to embark upon proposing SAM-PIE by applying the SAM's generated stability scores and masks. The regions of thermal anomalies in the original image can be spotted by the enhanced images, thereby providing the attention maps for the classification models for an enhanced classification of PV images. The techniques in the proposed SAM-PIE enable its effectiveness in inspection and analysis of thermal anomalies in solar cells of PV modules. The work carried out in this paper is a step towards automated inspection and analysis of thermal anomalies in solar cells of PV modules. The unique contributions of the proposed SAM-PIE method are as follows:

- Images of PV modules were originally collected, processed into datasets and publicly and freely available for scientific community use at https://doi.org/10.17632/5ssmfpgrpc.1
- Using drone (DJI Mavic 3 Thermal) for data collection addresses limitations in prior works that focused on collecting static images of PV modules. Moreover, this approach solves data limitations that could negatively influence the performance and accuracy of the proposed SAM-PIE.
- Integration of a novel PIE model into an existing SAM model to generate enhanced images for accurate classification of the thermal anomalies in solar cells of PV modules.

The rest of the paper's contents is as follows: Section II presents the related work. Section III presents the materials and methods. Section IV presents the experiments. Section V presents the results and discussions. Section VI concludes the study.

II. Related Work

Kirillov et al. [1] proposed a model called SAM model for the segmentation of any objects in an image. The model displayed great efficiency in fundamental instance segmentation task. Rafaeli et al. [2] applied SAM model 2 for a prompt-based segmentation at multiple resolutions and lighting conditions. Wang et al. [3] proposed an image enhancement based on SAM model that facilitates diagnosis of medical images. Lüddecke and Ecker [4] proposed in their work, a method based on text and image prompts for segmenting images. Mazurowski et al. [5] in their work, proposed an experimental study for analyzing medical images using SAM

model. Wang et al. [6] proposed a SAM model for scaling-up segmentation dataset of remote sensing. Feldman and Margolis [7] presented a report that contained update on industrial production and consumption of solar energy. Huang et al. [8], by considering dust impact, proposed a method for diagnosing PV faults based on a designed hybrid artificial bee colony algorithm and semi-supervised extreme learning machine. Cubukcu and Akanalci [9] proposed an inspection and determination methods in real-time of PV power systems faults by thermal imaging. Tsanakas et al. [10] proposed an advanced installation inspection method of PV by aerial triangulation and terrestrial georeferencing of thermal/visual imagery. Herraiz et al. [11] proposed thermal images analysis through structure based on CNNs for PV plant condition monitoring. Cheng et al. [12] employed self-adaptive chaos particle swarm optimization algorithm for the extraction of solar cell model parameters. Yang et al. [13] proposed a perfectly consistent and coherent transition from classification to segmentation using a novel SAM-based weakly-supervised method with a case study in latent PV locations segmentation. Pei and Hao [14] used voltage and current observation and evaluation method in their proposed PV systems to detect a fault. Georgijevic et al. [15] employed arc current entropy for detecting series arc fault in PV systems. Zhao et al. [16] presented a fault analysis method and protection challenges for solar PV arrays based on line-line fault analysis. Hariharan et al [17] proposed a method for detecting in PV systems, partial shading and other faults in PV array. Pillai and Rajasekar [18] proposed a sensorless line-line and line-ground technique based on MPPT for detecting faults for PV systems. Kurukuru et al. [19] proposed a novel approach for PV systems designed for fault classification. Chine et al. [20] proposed a novel method for diagnosing fault for PV systems based on artificial neural networks (ANNs). Hussain et al. [21] proposed a method integrating two bi-directional input parameters driven by ANN for detecting PV fault. Vieira et al. [22] proposed a method for detecting faults in PV systems by comparing multilayer perceptron and probabilistic neural network. Yuan et al. [23] conducted a survey on ANN for solar PV systems fault diagnosis. Hichri et al. [24] applied genetic-algorithm-based neural network to grid-connected PV systems for fault detection and diagnosis. Zhu et al. [25] proposed an approach based on unsupervised sample clustering and probabilistic neural network model for diagnosing fault for PV arrays. Eskandari et al. [26] proposed an autonomous fault diagnosis method based on weighted ensemble learning for PV systems using genetic algorithm. Wang et al. [27] proposed a support vector machine method for diagnosing PV array fault. Ravi et al. [28] proposed a Sam 2, a SAM model for segmenting anything in images and videos. Bommasani et al. [29] presented a work on the advantages and disadvantages of foundation models. Badr et al. [30] proposed a machine learning classifiers for identifying PV array fault. Lu et al. [31] proposed a CNN and electrical time series graph for diagnosing PV array fault. Liu et al. [32] proposed an approach based on stacked auto-encoder and clustering with IV curves for diagnosing PV array fault. Mellit [33] proposed a method based on thermographic images and deep CNNs as embedded solution for detecting and diagnosing PV module fault. He et al. [34] proposed a deep residual learning method for recognizing images. Bello et al. [35] proposed a PVMD dataset for automated detection and analysis of fault in large PV systems using PV module fault detection.

III. Materials and Methods

A. Data Collection and Description

The main hardware materials employed in this study comprise the hardware components for collecting and processing the data used in performing the experiment in this study. The materials are: (1) DJI Mavic 3 Thermal which is a state-of-the-art drone specifically designed for thermal imaging and inspection tasks, (2) Solar panels, (3) PV modules which include two panels of Jinko JKM200M-72 modules, each producing 200 W, (4) Inverter, (5) Storage battery, (6) DC Load, and (7) Solar charge controller. Table I shows the PVMD Dataset with the number of images in each anomaly category.

Popular PV image classification models, ResNet50 and CNNs were employed in carrying out the experiments of this study with one thousand PV module datasets [35], a Mendeley data comprising Hotspots (350 thermal generated images), Cracks (350 thermal generated images) and Shadings (300 thermal generated images). Afterward, we partitioned the dataset into training dataset (80%) and testing dataset (20%) to ease model evaluation. The images were pre-processed to standard size dimensions, and normalization techniques were applied for dataset consistency.

Additionally, the RGB images which were originally of different dimensions due to unfriendly and unstable environmental conditions were trimmed to size 512x512x3 (3 keeps the color information) and augmented using augmentation techniques such as geometric transformation, color-based transformations, illumination transformation, noise injection, etc., for dataset robustness.

Fig. 1 shows the framework of PV image classification with SAM-enabled PV-module image enhancement (SAM-PIE). The Fig. 1 shows the step-by-step process comparing the PV image classification output with SAM-PIE and without SAM-PIE.

TABLE I. PVMD Dataset with the Number of Images in Each Anomaly Category [35]

Thermal Anomaly of PV Module	Number of images
Hotspots	350
Cracks	350
Shadings	300
Total	**1000**

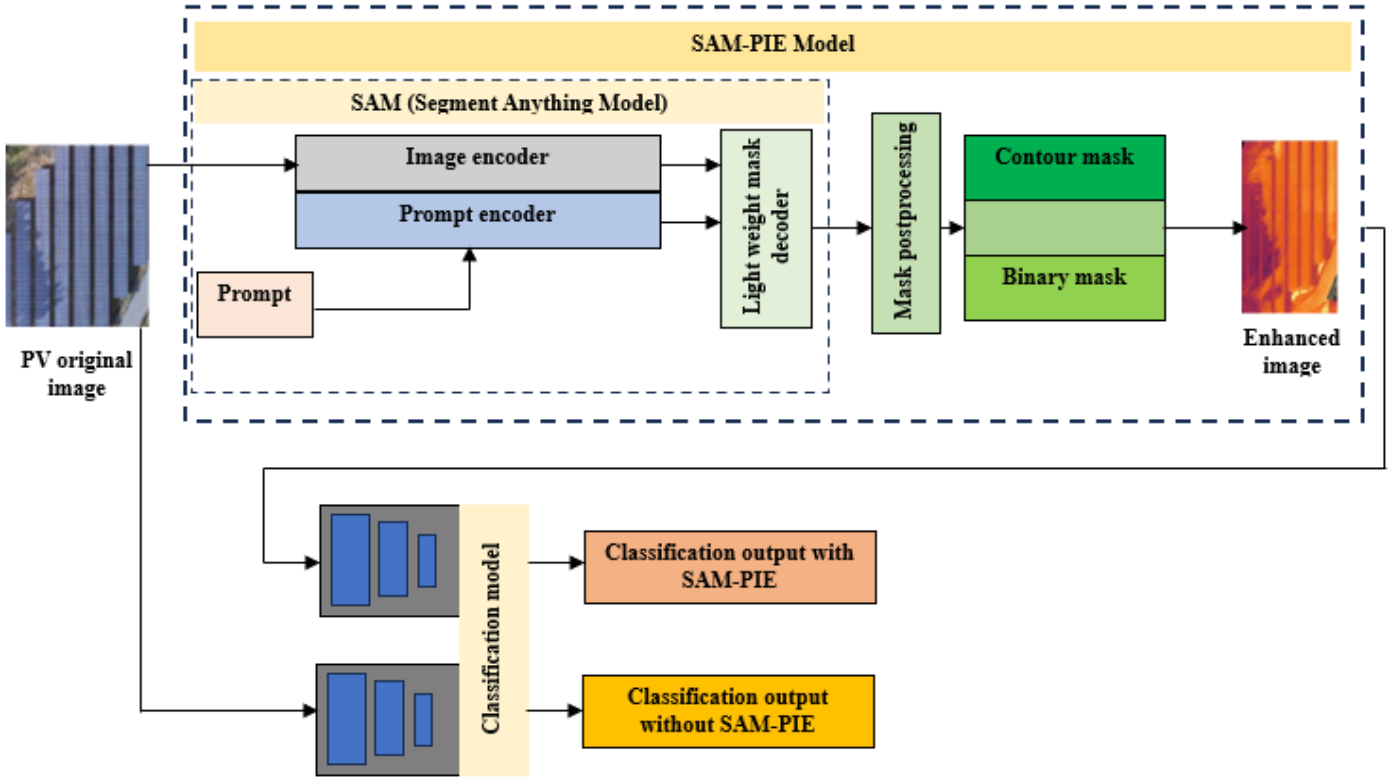

Fig. 1. The proposed framework of PV image classification with SAM-enabled PV-module image enhancement (SAM-PIE).

B. Image Processing Methods

The foundation of this study lies in the utilization of image processing techniques to detect and analyze faults in large PV systems. High-resolution images of PV panels are captured using drones equipped with advanced imaging sensors. These images undergo a series of preprocessing steps, including noise reduction, contrast enhancement, and normalization, to prepare the data for further analysis. The primary method for fault detection is based on the identification of anomalies such as cracks, hotspots, and shadings effects within the images. CV classification models, including ResNet50 and CNNs are employed to highlight these anomalies. Specifically, SAM-PIE method is used to improve the visibility of potential faults.

PV image segmentation method of SAM-PIE is applied to isolate areas of interest, facilitating targeted analysis. Once the segmentation is complete, each segment is analyzed using pattern recognition and classification algorithms to determine the presence and type of fault. The system is designed to operate unsupervised, utilizing machine learning models trained on a diverse dataset of labeled fault types. This approach allows for the automatic classification of detected faults without the need for manual intervention, significantly reducing the time and effort required for maintenance. Fig. 2 shows the hardware components used in developing the system.

C. Video Processing Methods

In addition to image processing, video processing is implemented to provide a comprehensive overview of the PV system's health. Drones equipped with video cameras capture continuous footage of the solar panels, which is then processed frame-by-frame to detect dynamic changes and faults that may not be visible in still images. The video processing workflow begins with the extraction of key frames from the video feed, focusing on frames that show significant changes or potential faults. These key frames are processed using similar techniques used in image processing. However, video processing also allows for the analysis of temporal changes, such as the progression of hotspots or the spread of shadings over time. To enhance the fault detection process, motion detection and tracking algorithms are used to follow up anomalies across multiple frames. This enables the system to monitor the development of faults and assess their impact on the overall performance of the PV system.

The combination of image and video processing ensures a more robust and reliable fault detection mechanism, capable of adapting to varying environmental conditions and operational challenges. As illustrated in Fig. 2, the deployment of a DJI Mavic 3 drone, equipped with a thermal camera, captures the detailed images and videos of a solar PV array. The drone flies over the solar installation, systematically collecting visual data that reveals the thermal characteristics of the PV panels. This data is then transferred to a computer where a specialized application (proposed in this paper) processes the images and videos. The processing involves analyzing the thermal data to detect anomalies such as hotspots, cracks, and shadings issues, which are indicative of faults in the solar panels. This method provides a comprehensive and efficient approach to monitoring and maintaining large PV systems. The drone is equipped with a thermal camera to record the condition of the solar panels.

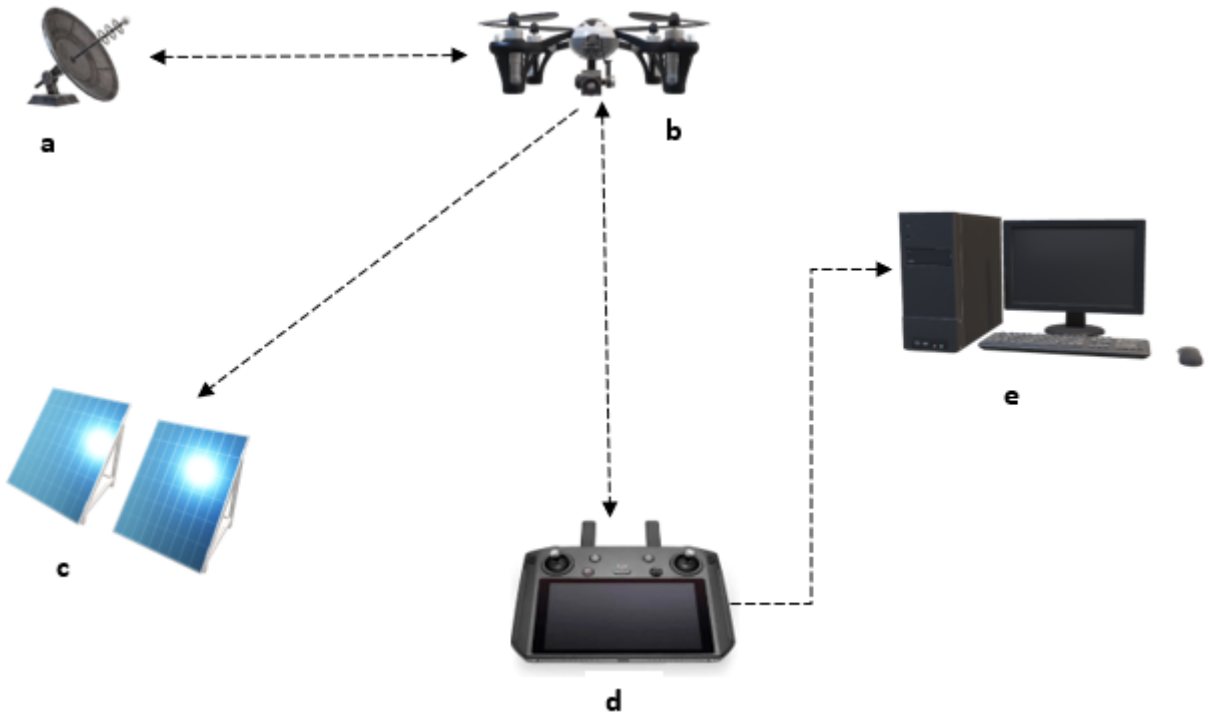

Fig. 2. System description showing the hardware components for (a) Satellite, (b) DJI Mavic 3 Thermal drone, (c) PV, (d) Remote control, (e) Computer system.

The drone captures thermal images and videos of the PV array, collecting comprehensive data on the surface temperature and potential anomalies across the solar panels. After capturing the necessary data, the drone transmits the thermal images and videos to a computer for further processing and analysis. The transferred data undergoes preprocessing, which includes steps like noise reduction and normalization to enhance the quality and clarity of the images and videos, making them suitable for analysis. Machine vision algorithms (proposed in this paper) are applied to the preprocessed data to detect any anomalies, such as hotspots, cracks, or shadings that might indicate faults in the PV panels.

D. Image Enhancement and Classification Models

Applying the pre-trained SAM enables the segmentation masks generation for PV images, and the segmentation masks (including stability scores) can be generated by SAM for the whole regions in a PV image with no antecedent prompts; binary mask and contour mask are also generated, this is followed by a procedure performed to generate enhanced images as evident in Fig. 1 and Fig. 3. Two types of segmentation tasks are involved when segmenting PV images; the foreground (that contains region of object) and the background. Given the following set as the original training dataset $\{(p_1, q_1), (p_2, q_2), (p_3, q_3), \ldots, (p_n, q_n)\}$, where the classification label of the PV image p_i is denoted as $p_i \in \mathbb{R}^{w \times h \times 3}$, $q_1 \in \{0, 1\}$. By the application of SAM-PIE method to each image of PV in the training set, the following set is generated as a new enhanced training dataset: $\{(p_1^{PIE}, q_1), (p_2^{PIE}, q_2), (p_3^{PIE}, q_3), \ldots, (p_n^{PIE}, q_n)\}$, where $p_i^{PIE} \in \mathbb{R}^{w \times h \times 3}$ is the enhanced image p_i of PV. ResNet50 and CNNs (denoted as M) were applied in order to learn from training sets that were not enhanced by SAM-PIE; optimization of the parameters of M is as follows:

$$\sum_{i=1}^{n} loss(M(p_i), q_i) \quad (1)$$

In essence, to minimize the target based on M parameters is the new learning objective:

$$\sum_{i=1}^{n} \alpha loss(M(p_i), q_i) + \theta loss(M(p_i^{PIE}), q_i) \quad (2)$$

Where α and θ put under check the training loss value for original and enhanced images; Eq. (2) would be simplified to Eq. (1) when α=1 and θ=0. However, in this paper, both α and θ take the same number 1, in order to assign equal weight to both original and enhan ced images. Cross-entropy loss was employed for the construction of loss function (expressed in Eq. (1) and Eq. (2)). Eq. (3) is used for testing the model as follows:

$$q = f\left(M(p)\right) \quad (3)$$

where f the sigmoid output activation function.

IV. EXPERIMENTS

A. Implementation Details and Evaluation Metrics

The main software materials employed to process the images and the videos are: (1) Python 3.x on a Windows 11 Home, along with libraries such as Flask, OpenCV, NumPy, Matplotlib, Google Colab and GPU for training the model, (2) CV classification models, including ResNet50 and CNNs. The initial learning rate of 0.01 was set for ResNet50, with batch size fixed at 70; the initial learning rate of 0.001 was set for CNNs, with batch size fixed at 40. The classification experiment was conducted on all the original datasets and the performance compared with the performance of the classification experiment conducted on SAM-PIE enhanced datasets.

In this paper, the performance of the proposed method was evaluated using the evaluation metrics in terms of Precision, Average Precision (AP), and Recall. Precision is denoted by Eq. (4), Recall is denoted by Eq. (5), AP is denoted by Eq. (6), IOU, which stands for Intersection Over Union is denoted by Eq. (7). The analysis stage involves evaluating the detected faults, determining their types, and pinpointing their exact locations on the solar panels. The results of the analysis would be compiled into a comprehensive report. This report not only includes the identified faults and their locations but also suggests potential maintenance actions to address the detected issues.

$$P = \frac{True\ positive}{True\ positive + False\ positive} \quad (4)$$

$$R = \frac{True\ positive}{True\ positive + False\ negative} \quad (5)$$

$$AP = \sum_{n=1}^{N} [R(n) - R(n-1)].maxP(n) \quad (6)$$

Where, N is the number for PR points calculate

$$IOU = \frac{A \cap B}{A\ U\ B} \times 100 \quad (7)$$

Where, f is the sigmoid output activation function.

V. Results and Discussions

A. Results

This study achieved the image enhancement solution for PV thermal Hotspots, PV thermal Shadings, and PV thermal Cracks datasets with the aid of SAM-PIE; this is shown in Fig. 3, which depicts the original images and the enhanced images by SAM-PIE (the processed contour and binary masks resulted in enhanced images).

The performance of the classification experiment conducted on all the original datasets was compared with the performance of the classification experiment conducted on SAM-PIE enhanced datasets. Table II shows the results of the classification task on three datasets, namely Hotspots, Cracks, and Shadings.

The results obtained in this study support SAM performance as a fundamental model that has produced significant achievements in natural image segmentation tasks, even with more better results if well guided for prompt-able segmentation. SAM's performance in segmentation tasks involving PV images is below par with the best due to the dissimilarity between images of solar cells of PV modules and natural images. The performance of SAM's application in PV image segmentation tasks remains a topic of public interest. Fig. 4 shows the graphical results of ResNet50 and CNNs classification models on original Hotspot thermal anomaly dataset and SAM-PIE enhanced Hotspot thermal anomaly dataset. The metrics measure the classification accuracy of the ResNet50 and CNNs classification models on original Hotspot thermal anomaly dataset and SAM-PIE enhanced Hotspot thermal anomaly dataset.

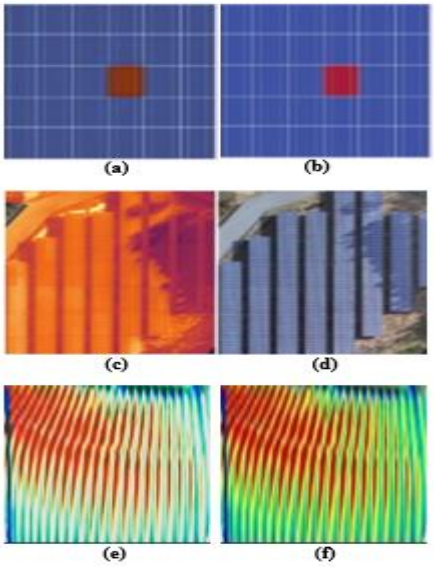

Fig. 3. Image segmentation showing (a) raw image of thermal Hotspot, (b) SAM-PIE enhanced image of thermal Hotspot, (c) raw image of thermal Shading, (d) SAM-PIE enhanced image of thermal Shading, (e) raw image of thermal Crack, (f) SAM-PIE enhanced image of thermal Crack.

TABLE II. The Results of ResNet50 and CNNs Classification Models on Original Three Thermal Anomaly Datasets (Hotspots, Cracks, and Shadings) and SAM-PIE Enhanced Three Thermal Anomaly Datasets (Hotspots, Cracks, and Shadings)

Dataset	Model	AUC	Accuracy	Precision	Recall	F1 score
Hotspot	CNNs	0.906	0.778	0.756	0.900	0.828
	ResNet50	0.958	0.889	0.789	0.915	0.852
	CNNs with SAM-PIE	0.964	0.878	0.766	0.910	0.838
	ResNet50 with SAM-PIE	0.966	0.891	0.847	0.955	0.901
Crack	CNNs	0.899	0.776	0.750	0.888	0.826
	ResNet50	0.950	0.879	0.788	0.910	0.848
	CNNs with SAM-PIE	0.962	0.878	0.764	0.905	0.834
	ResNet50 with SAM-PIE	0.964	0.895	0.795	0.945	0.870
Shading	CNNs	0.850	0.766	0.735	0.824	0.826
	ResNet50	0.940	0.877	0.768	0.915	0.848
	CNNs with SAM-PIE	0.955	0.855	0.765	0.895	0.830
	ResNet50 with SAM-PIE	0.955	0.890	0.785	0.935	0.860

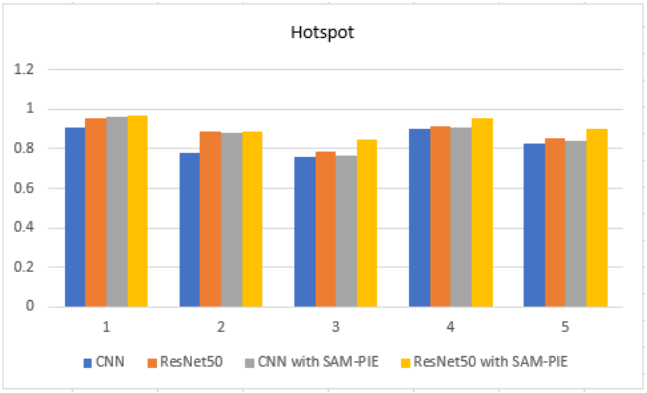

Fig. 4. Graphical results of ResNet50 and CNNs classification models on original Hotspot thermal anomaly dataset and SAM-PIE enhanced Hotspot thermal anomaly dataset.

The solar cells of PV modules are not among the natural images covered in SAM datasets, making it difficult for SAM to be applied to the PV image segmentation task, however, the experimental evidence shows that the performance of SAM, although may not be excellent on solar cells image segmentation, it could perform excellently well on region of thermal anomaly (region of interest) in an image by adjusting the confidence level of the region segmented. In PV fault diagnosis, whether during installation, repair or maintenance, the anomalies occurrence in solar cells of the PV modules are often traced to changes in their morphologies and other components due to environmental factors, making it worthy to apply SAM for the extraction of those regions of interest in this paper. Fig. 5 shows the graphical results of ResNet50 and CNNs classification models on original Crack thermal anomaly dataset and SAM-PIE enhanced Crack thermal anomaly dataset. The metrics measure the classification accuracy of the ResNet50 and CNNs classification models on original Crack thermal anomaly dataset and SAM-PIE enhanced Crack thermal anomaly dataset.

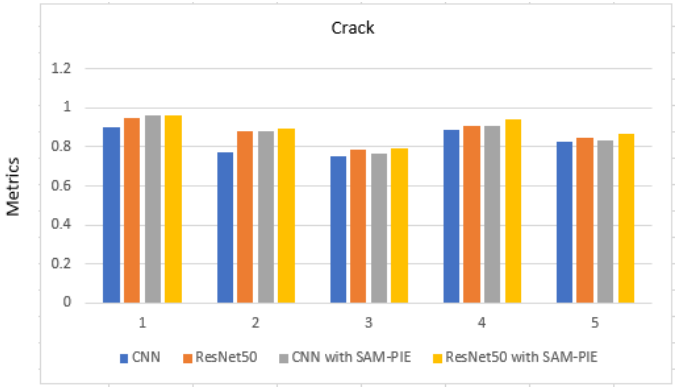

Fig. 5. Graphical results of ResNet50 and CNNs classification models on original Crack thermal anomaly dataset and SAM-PIE enhanced Crack thermal anomaly dataset.

According to Table II, the classification results obtained by ResNet50 and CNNs classification models with SAM-PIE enhanced images in AUC, Accuracy, Precision, Recall, and F1 score were higher than the results obtained by ResNet50 and CNNs classification models without SAM-PIE enhanced images. Moreover, according to Fig. 3, SAM-PIE performed excellently well on image enhancement of raw images of thermal Hotspot, thermal Shading, and thermal Crack as presented in Fig. 3 (a) to Fig. 3 (f).

These results were influenced by the characteristics of individual thermal anomalies. Although SAM-PIE produced promising results, it faced some performance challenges and compromise in enhancing some regions of interest on the image due to unrevealed external information in the image. Fig. 6 shows the graphical results of ResNet50 and CNNs classification models on original Shading thermal anomaly dataset and SAM-PIE enhanced Shading thermal anomaly dataset. The metrics measure the classification accuracy of the ResNet50 and CNNs classification models on original Shading thermal anomaly dataset and SAM-PIE enhanced Shading thermal anomaly dataset.

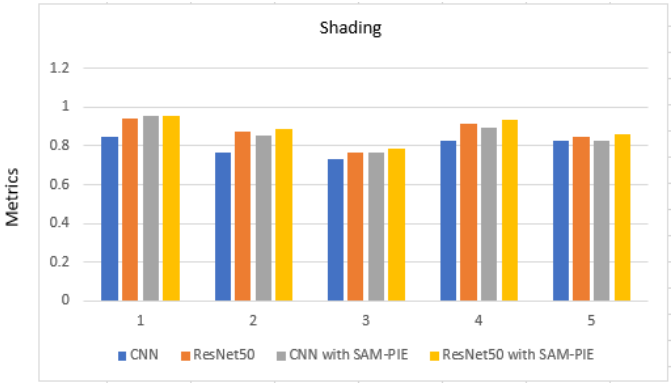

Fig. 6. Graphical results of ResNet50 and CNNs classification models on original Hotspot Graphical results of ResNet50 and CNNs classification models on original Shading thermal anomaly dataset and SAM-PIE enhanced Shading thermal anomaly dataset.

B. Discussions

Table II shows the results of ResNet50 and CNNs classification models on original three thermal anomaly datasets (hotspots, cracks, and shadings) and SAM-PIE enhanced three thermal anomaly datasets (hotspots, cracks, and shadings). These results were compared with similar previous work. The findings from the result obtained in Huang et al. [8] validate the effectiveness of SAM-PIE proposed in this study for diagnosing PV faults. The thermal imaging applied in Cubukcu and Akanalci [9] produced results that also validate the results generated by the drone used in this study to inspect and determine PV power systems faults in real-time. The advanced installation inspection method employed in Tsanakas et al. [10] for PV systems produced results that are on a par with the results produced in Herraiz et al. [11], who applied thermal images analysis through structure based on CNNs for PV plant condition monitoring. However, the performance of the thermal images applied in [10] and [11] was less accurate than the performance obtained in this study for anomaly classification of hotspots, cracks and shadings. The application of the proposed SAM-PIE in this study performed better than the method applied in Cheng et al. [12] for the extraction of solar cell model parameters. The novel SAM-based weakly-supervised method applied in Yang et al. [13], though showed promising results, however, their approach in transiting from classification to segmentation of latent PV locations

segmentation did not extensively cover the thermal anomalies studied in this work. Moreover, the SAM model on which their experiment was based does not have the prompts capability for panoptic and semantic segmentation implementation. The voltage and current observation and evaluation method used in Pei and Hao [14] to detect a fault in PV systems had limitations in its application to hotspots, cracks, and shadings thermal anomalies detection. The results obtained in Georgijevic et al. [15] were on a par with the results obtained in Zhao et al. [16] for detecting fault in PV systems. Their results were in contrast to the results obtained in this study and this is due to the difference in method employed and problem addressed. The problem addressed and the results obtained in Hariharan et al [17] were similar to the problem and results obtained in this study except for the methods. In this study, we addressed and detected full shadings in PV systems, however, partial shading was addressed in [17]. The sensorless line-line and line-ground technique based on MPPT used in Pillai and Rajasekar [18] could not give accurate account of the three anomalies addressed in this study, which are the main challenges faced by PV systems. The method applied in this study are similar to the method employed in Chine et al. [20], Hussain et al. [21], Vieira et al. [22], and Yuan et al. [23] with promising results obtained. The method, CNN and electrical time series graph, used in Lu et al. [31] for diagnosing PV array fault was partially similar to the method used in this study except for the electrical time series graph. However, the classification results of the diagnosed PV array fault were not as accurate as the results obtained in this study. An important factor that distinguished SAM-PIE from the traditional IE methods is the low-level in which the traditional IE methods frequently work, which is below the high-level requirement for reconstructing and recovering an original image [5], which is what SAM-PIE achieved in this study.

VI. Conclusion

SAM-enabled photovoltaic-module image enhancement (SAM-PIE) for fault inspection and analysis using ResNet50 and CNNs has been proposed in this paper. The results from the classification experiments were obtained from three different publicly available thermal anomaly datasets of PV modules, which also validate SAM-PIE efficiency and performance in image enhancement for PV image classification tasks by classification models.

However, SAM-PIE faces some performance challenges and compromise in enhancing some regions of interest on the image due to unrevealed external information in the image. To improve on SAM-PIE limitations for PV image classification, it is part of our future work to employ more practicable tactics such as integrating SAM-PIE into more different PV image classification models or related tasks, for instance.

References

[1] A. Kirillov, E. Mintun, N. Ravi, H. Mao, C. Rolland, L. Gustafson, ... and R. Girshick, "Segment anything," In Proceedings of the IEEE/CVF International Conference on Computer Vision, pp. 4015-4026, 2023.

[2] O. Rafaeli, T. Svoray, and A. Nahlieli, "Prompt-Based segmentation at multiple resolutions and lighting conditions using segment anything model 2," arXiv preprint arXiv:2408.06970, 2024.

[3] C. Wang, H. Chen, X. Zhou, M. Wang, and Q. Zhang, "SAM-IE: SAM-based image enhancement for facilitating medical image diagnosis with segmentation foundation model," Expert Systems with Applications, pp. vol. 249, pp. 123795, 2024.

[4] T. Lüddecke, and A. Ecker, "Image segmentation using text and image prompts," In Proceedings of the IEEE/CVF Conference on Computer Vision and Pattern Recognition, pp. 7086-7096, 2022.

[5] M. A. Mazurowski, H. Dong, H. Gu, J. Yang, N. Konz, and Y. Zhang, "Segment anything model for medical image analysis: an experimental study," Medical Image Analysis, vol. 89, pp. 102918, 2023.

[6] D. Wang, J. Zhang, B. Du, M. Xu, L. Liu, D. Tao, and L. Zhang, "Samrs: Scaling-up remote sensing segmentation dataset with segment anything model," Advances in Neural Information Processing Systems, vol. 36, 2024.

[7] D. J. Feldman, and R. M. Margolis, "Q4 2018/Q1 2019 Solar industry update [Slides] (No. NREL/PR-6A20-73992)," National Renewable Energy Laboratory (NREL), Golden, CO (United States), 2019.

[8] J. M. Huang, R. J. Wai, and G. J. Yang, "Design of hybrid artificial bee colony algorithm and semi-supervised extreme learning machine for PV fault diagnoses by considering dust impact," IEEE Transactions on Power Electronics, vol. 35, No. 7, pp. 7086-7099, 2019.

[9] M. E. T. E. Cubukcu, and A. Akanalci, "Real-time inspection and determination methods of faults on photovoltaic power systems by thermal imaging in Turkey," Renewable Energy, vol. 147, pp. 1231-1238, 2020.

[10] J. A. Tsanakas, L. D. Ha, and F. Al Shakarchi, "Advanced inspection of photovoltaic installations by aerial triangulation and terrestrial georeferencing of thermal/visual imagery," Renewable Energy, vol. 102, pp. 224-233, 2017.

[11] A. H. Herraiz, A. P. Marugán, and F. P. G. Márquez, "Photovoltaic plant condition monitoring using thermal images analysis by convolutional neural network-based structure," Renewable Energy, vol. 153, pp. 334-348, 2020.

[12] Z. Cheng, M. N. Dong, T. K. Yang, and L. J. Han, "Extraction of solar cell model parameters based on self-adaptive chaos particle swarm optimization algorithm," Transactions of China Electrotechnical Society, vol. 29, No. 9, pp. 245-252, 2014.

[13] R. Yang, G. He, R. Yin, G. Wang, Z. Zhang, T. Long, ... and J. Wang, "A novel weakly-supervised method based on the segment anything model for seamless transition from classification to segmentation: A case study in segmenting latent photovoltaic locations," International Journal of Applied Earth Observation and Geoinformation, vol. 130, pp. 103929, 2024.

[14] T. Pei, and X. Hao, "A fault detection method for photovoltaic systems based on voltage and current observation and evaluation," Energies, vol. 12, No. 9, pp. 1712, 2019.

[15] N. L. Georgijevic, M. V. Jankovic, S. Srdic, and Z. Radakovic, "The detection of series arc fault in photovoltaic systems based on the arc current entropy," IEEE Transactions on Power Electronics, vol. 31, No. 8, pp. 5917-5930, 2015.

[16] Y. Zhao, J. F. De Palma, J. Mosesian, R. Lyons, and B. Lehman, "Line–line fault analysis and protection challenges in solar photovoltaic arrays," IEEE transactions on Industrial Electronics, vol. 60, No. 9, pp. 3784-3795, 2012.

[17] R. Hariharan, M. Chakkarapani, G. S. Ilango, and C. Nagamani, "A method to detect photovoltaic array faults and partial shading in PV systems," IEEE Journal of Photovoltaics, vol. 6, No. 5, pp. 1278-1285, 2016.

[18] D. S. Pillai, and N. Rajasekar, "An MPPT-based sensorless line–line and line–ground fault detection technique for PV systems," IEEE Transactions on Power Electronics, vol. 34, No. 9, pp. 8646-8659, 2018.

[19] V. S. B. Kurukuru, F. Blaabjerg, M. A. Khan, and A. Haque, "A novel fault classification approach for photovoltaic systems," Energies, vol. 13 No. 2, pp. 308, 2020.

[20] W. Chine, A. Mellit, V. Lughi, A. Malek, G. Sulligoi, and A. M. Pavan, "A novel fault diagnosis technique for photovoltaic systems based on artificial neural networks," Renewable Energy, vol. 90, pp. 501-512, 2016.

[21] M. Hussain, M. Dhimish, S. Titarenko, and P. Mather, "Artificial neural network based photovoltaic fault detection algorithm integrating two bi-

directional input parameters," Renewable Energy, vol. 155, pp. 1272-1292, 2020.

[22] R. G. Vieira, M. Dhimish, F. M. U. de Araújo, and M. I. da Silva Guerra, "Comparing multilayer perceptron and probabilistic neural network for PV systems fault detection," Expert Systems with Applications, vol. 201, pp. 117248, 2022.

[23] Z. Yuan, G. Xiong, and X. Fu, "Artificial neural network for fault diagnosis of solar photovoltaic systems: a survey," Energies, vol. 15, No. 22, pp. 8693, 2022.

[24] A. Hichri, M. Hajji, M. Mansouri, K. Abodayeh, K. Bouzrara, H. Nounou, and M. Nounou, "Genetic-algorithm-based neural network for fault detection and diagnosis: Application to grid-connected photovoltaic systems," Sustainability, vol. 14 No. 17, pp. 10518, 2022.

[25] H. Zhu, L. Lu, J. Yao, S. Dai, and Y. Hu, "Fault diagnosis approach for photovoltaic arrays based on unsupervised sample clustering and probabilistic neural network model," Solar Energy, vol. 176, pp. 395-405, 2018.

[26] A. Eskandari, M. Aghaei, J. Milimonfared, and A. Nedaei, "A weighted ensemble learning-based autonomous fault diagnosis method for photovoltaic systems using genetic algorithm," International Journal of Electrical Power & Energy Systems, vol. 144, pp. 108591, 2023.

[27] J. Wang, D. Gao, S. Zhu, S. Wang, and H. Liu, "Fault diagnosis method of photovoltaic array based on support vector machine," Energy sources, part a: recovery, utilization, and environmental effects, vol. 45 No. 2, pp. 5380-5395, 2023.

[28] N. Ravi, V. Gabeur, Y. T. Hu, R. Hu, C. Ryali, T. Ma, ... and C. Feichtenhofer, "Sam 2: Segment anything in images and videos," arXiv preprint arXiv:2408.00714, 2024.

[29] R. Bommasani, D. A. Hudson, E. Adeli, R. Altman, S. Arora, S. von Arx, ... and P. Liang, "On the opportunities and risks of foundation models," arXiv preprint arXiv:2108.07258, 2021.

[30] M. M. Badr, M. S. Hamad, A. S. Abdel-Khalik, R. A. Hamdy, S. Ahmed, and E. Hamdan, "Fault identification of photovoltaic array based on machine learning classifiers," IEEE Access, vol. 9, pp. 159113-159132, 2021.

[31] X. Lu, P. Lin, S. Cheng, Y. Lin, Z. Chen, L. Wu, and Q. Zheng, "Fault diagnosis for photovoltaic array based on convolutional neural network and electrical time series graph," Energy Conversion and Management, vol. 196, pp. 950-965, 2019.

[32] Y. Liu, K. Ding, J. Zhang, Y. Li, Z. Yang, W. Zheng, and X. Chen, "Fault diagnosis approach for photovoltaic array based on the stacked auto-encoder and clustering with IV curves," Energy Conversion and Management, vol. 245, pp. 114603, 2021.

[33] A. Mellit, "An embedded solution for fault detection and diagnosis of photovoltaic modules using thermographic images and deep convolutional neural networks," Engineering Applications of Artificial Intelligence, vol. 116, pp. 105459, 2022.

[34] K. He, X. Zhang, S. Ren, and J. Sun, "Deep residual learning for image recognition," In Proceedings of the IEEE Conference on Computer Vision and Pattern Recognition, pp. 770-778, 2016.

[35] R. W. Bello, P. A. Owolawi, E. A. Van Wyk, and C. Du, "Photovoltaic module dataset for automated fault detection and analysis in large photovoltaic systems using photovoltaic module fault detection," Mendeley Data, V1, https://doi.org/10.17632/5ssmfpgrpc.1, 2024.